

Alma Mater Studiorum Università di Bologna
Archivio istituzionale della ricerca

Classification of cow diet based on milk Mid Infrared Spectra: A data analysis competition at the “International Workshop on Spectroscopy and Chemometrics 2022”

This is the final peer-reviewed author’s accepted manuscript (postprint) of the following publication:

Published Version:

Maria Frizzarin, G.V. (2023). Classification of cow diet based on milk Mid Infrared Spectra: A data analysis competition at the “International Workshop on Spectroscopy and Chemometrics 2022”. CHEMOMETRICS AND INTELLIGENT LABORATORY SYSTEMS, 234(15 March 2023), 1-13 [10.1016/j.chemolab.2023.104755].

Availability:

This version is available at: <https://hdl.handle.net/11585/912489> since: 2023-07-24

Published:

DOI: <http://doi.org/10.1016/j.chemolab.2023.104755>

Terms of use:

Some rights reserved. The terms and conditions for the reuse of this version of the manuscript are specified in the publishing policy. For all terms of use and more information see the publisher's website.

This item was downloaded from IRIS Università di Bologna (<https://cris.unibo.it/>).
When citing, please refer to the published version.

(Article begins on next page)

1 CLASSIFICATION OF COW DIET BASED ON MILK MID
2 INFRARED SPECTRA: A DATA ANALYSIS COMPETITION
3 AT THE “INTERNATIONAL WORKSHOP ON
4 SPECTROSCOPY AND CHEMOMETRICS 2022”

5 Maria Frizzarin^{1,2}, Giulio Visentin^{*3}, Alessandro Ferragina⁴, Elena Hayes⁵, Antonio
6 Bevilacqua⁶, Bhaskar Dhariyal⁶, Katarina Domijan⁷, Hussain Khan⁴, Georgiana Ifrim⁶,
7 Thach Le Nguyen⁶, Joe Meagher^{2,8}, Laura Menchetti⁹, Ashish Singh⁶, Suzy
8 Whoriskey^{2,8}, Robert Williamson¹⁰, Martina Zappaterra¹¹, and Alessandro Casa¹²

9 ¹*Teagasc, Animal & Grassland Research and Innovation Centre, Moorepark, Ireland*

10 ²*School of Mathematics and Statistics, University College Dublin, Ireland*

11 ³*Department of Veterinary Medical Sciences, University of Bologna, Italy*

12 ⁴*Teagasc Food Research Centre, Ashtown, Ireland*

13 ⁵*Teagasc, Food Research Centre, Moorepark, Ireland*

14 ⁶*School of Computer Science, University College Dublin, Ireland*

15 ⁷*Department of Mathematics and Statistics, National University of Ireland, Maynooth, Ireland*

16 ⁸*Insight Centre for Data Analytics, University College Dublin, Ireland*

17 ⁹*School of Biosciences and Veterinary Medicine, University of Camerino, Italy*

18 ¹⁰*School of Electronics, Electrical Engineering and Computer Science, Queen's University Belfast, UK*

19 ¹¹*Department of Agricultural and Food Sciences, University of Bologna, Italy*

20 ¹²*Faculty of Economics and Management, Free University of Bozen-Bolzano, Italy*

21 **Abstract**

22 In April 2022, the Vistamilk SFI Research Centre organized the second edition of the
23 “International Workshop on Spectroscopy and Chemometrics – Applications in Food and
24 Agriculture”. Within this event, a data challenge was organized among participants of the
25 workshop. Such data competition aimed at developing a prediction model to discriminate
26 dairy cows’ diet based on milk spectral information collected in the mid-infrared region. In
27 fact, the development of an accurate and reliable discriminant model for dairy cows’ diet can
28 provide important authentication tools for dairy processors to guarantee product origin for
29 dairy food manufacturers from grass-fed animals. Different statistical and machine learning
30 modelling approaches have been employed during the workshop, with different pre-processing
31 steps involved and different degree of complexity. The present paper aims to describe the
32 statistical methods adopted by participants to develop such classification model.

33 **Keywords:** Chemometrics, Fourier transform mid-infrared spectroscopy, machine learning,
34 milk quality, food authenticity

35 **1 Introduction**

36 The use of mid-infrared spectroscopy (MIRS) has become a relevant topic in agri-food sciences,
37 due to its capacity to routinely quantify a wide range of important characteristics rapidly and
38 cost-effective. In particular, MIRS is nowadays commonly employed to monitor and quantify

*Corresponding author: address. Email: giulio.visentin@unibo.it

39 milk quality parameters, such as concentrations of fat, protein, casein, and lactose. These
40 parameters are used for milk quality-based payment schemes, genetic and genomic selection,
41 and as farmers’ support tool. Spectral information generated from MIRS analysis have also
42 proven to be effective in predicting fine milk quality parameters, including protein fractions,
43 free amino acids [Bonfatti et al., 2011; McDermott et al., 2016], individual and groups of fatty
44 acids [Soyeurt et al., 2006; Fleming et al., 2017], milk processing traits [Ferragina et al., 2013;
45 Visentin et al., 2015], animal-related characteristics [McParland et al., 2014; Shetty et al., 2017;
46 Ho et al., 2019], and can be used as a tool for the verification of the authenticity of agricultural
47 foods [Cozzolino, 2012]. A more extended list of applications of MIRS in the dairy science
48 framework can be retrieved from the reviews by De Marchi et al. [2014] and Tiplady et al.
49 [2020].

50 The two-day event “*International Workshop on Spectroscopy and Chemometrics*” was orga-
51 nized by Vistamilk SFI Research Centre in April 2022, following its first edition held in 2021
52 [Frizzarin et al., 2021a]. The workshop focused on describing the main challenges and appli-
53 cations of near and mid-infrared spectroscopy in food, animal, and agricultural sciences with
54 internationally recognised researchers. Moreover, participants, on a voluntary basis, were pro-
55 vided with a large dataset containing individual cow milk spectra with the sole information on
56 animal’s diet for a chemometric data competition. Such data presented many challenges from
57 a methodological and statistical point of view, due to the high dimensionality of the spectral
58 matrices, and strong collinearity between adjacent spectral wavelengths. The chemometric chal-
59 lenge, therefore, encouraged the engagement of participants with different background and skills
60 and required the application of different statistical and machine learning strategies.

61 The purpose of the data challenge was to develop a model to predict the diet fed to dairy
62 cows by exploiting mid-infrared spectral information. Participants, or groups of participants,
63 were required to apply their developed model to a test set containing only individual milk spectra
64 and to submit their prediction of animals’ diet. Since participation was found to be high, six
65 contributions out of twelve were selected, according to criteria based on the accuracy of the
66 predictions and methodological innovativeness, to present their results both at the workshop
67 and in the present manuscript.

68 2 Data description and challenge

69 A dataset consisting of 4,364 individual milk spectra from individual cows was collected between
70 May and August in 2015, 2016 and 2017 [O’Callaghan et al., 2016]. The samples were from Hol-
71 stein Friesian cows with different parity from Irish Dairy Research Herd in Teagasc Moorepark,
72 Fermoy, Co. Cork. Three dietary groups were evaluated with 54 cows being assigned to a di-
73 etary group each year. The three diet treatments were grass (GRS) which consisted of perennial
74 ryegrass only, clover (CLV) which consisted of perennial ryegrass with 20% annual clover sward,
75 and total mixed ration (TMR) where cows were fed grass silage, maize silage and concentrates
76 while being maintained indoors for the full season. Milk samples were collected in the morning
77 (AM) and evening (PM) milking session; subsequently AM+PM samples were pooled and anal-
78 ysed weekly using Pro-FOSS FT6000 (FOSS). The output spectrum contained a total of 1060
79 transmittance data points in the range from 925 cm^{-1} to $5,000\text{ cm}^{-1}$.

80 The dataset was divided into training (3275 spectra) and test (1089 spectra) data; for the
81 latter only spectral (i.e., independent variables) information was provided, while diet informa-
82 tion, to be used as a classification (i.e., dependent) variable, was available for the training set.
83 The training data included 1094 spectra for GRS, 1120 spectra from CLV and 1061 spectra for
84 TMR. There were no missing values in the training or test set. The specific information about
85 the wavenumbers had not been shared with the participants.

86 The three dietary groups were carefully selected based on their characteristics. As described
87 by Frizzarin et al. [2021b], pasture-based diets are easily discriminated from TMR diets, while

88 discriminating between GRS and CLV diets is much more difficult due to the similarities in the
89 sward composition resulting in similar milk composition. However, with the increased pressure
90 to reduce fertilizer use, and the introduction of multi-species swards, the development of a robust
91 discriminant model for classifying milk spectra based on diet is of paramount importance.

92 After the analysis, the participants submitted their predicted values for the test dataset and
93 a short explanation of the methodology used. The best methods were selected based on the
94 accuracy of the predictions for the test dataset. The accuracy was calculated as the proportion
95 of the correctly classified samples divided by the total number of samples in the test dataset.

96 3 Modelling approaches and results

97 3.1 Participant 1

98 The data were analyzed following different modelling strategies, focusing both on methods that
99 considered spectral proximity of the wavelengths and on methods that do not. All the analyses
100 have been mainly conducted using Python libraries `pandas`, `sklearn`, `sktime` and `matplotlib`
101 [see Pedregosa et al., 2011, and references therein]. The open source code is available at https://github.com/mlgig/vistamilk_diet_challenge and readers can refer to it for the specific
102 details about the implementation of all the methods outlined in this Section.
103

104 As a first step, some descriptive statistics were computed, and the outliers have been removed,
105 following both the recommendations given prior to the competition and a visual inspection of the
106 data. In the subsequent step, the labeled dataset was split according to a 3-fold cross-validation
107 (3CV) strategy. Therefore, the best model was selected based on cross-validation accuracy, and
108 then trained on the full training set and used to perform prediction on the provided unlabeled
109 test set.

110 In order to predict the diet, the following classification strategies were considered:

- 111 • **Tabular models:** each sample is considered as a vector of unordered features. In
112 particular, Ridge Classifier, where a penalty shrinking parameters towards zero is im-
113 posed on the coefficients of a logistic regression model [see e.g., Hoerl and Kennard,
114 1970], and Linear Discriminant Analysis (LDA) were tested. In the following, these
115 methods were coupled both with feature selection strategies and with random polynomial
116 feature transformations. The latter approach first used `sklearn` routines to create
117 new features (see, <https://scikit-learn.org/stable/modules/generated/sklearn.preprocessing.PolynomialFeatures.html>). For example, for features a, b, c , a poly-
118 nomial transformation of degree 2 will generate the features $1, a, b, c, ab, ac, bc, a^2, b^2, c^2$.
119 By generating these features, this approach aimed to check if non-linear interactions im-
120 proved the classification. Finally, a new approach (random polynomial transformation) is
121 presented, which aims to diversify the polynomial features (by random sampling) while
122 keeping low computational requirements.
123
- 124 • **Deep Neural Network Models:** a family of approaches based on deep neural networks,
125 both fully connected and convolutional, were tested. This strategy implicitly generates
126 complex features interactions, as captured by the network architecture.

127 Note that previously obtained results [Frizzarin et al., 2021a] suggest that tabular methods
128 work quite well with spectroscopy data. Moreover, following the suggestions in Frizzarin et al.
129 [2021b], feature selection strategies were coupled with the information about the presence of
130 water regions in the spectra. In addition, state-of-the-art time series classification algorithms,
131 such as ROCKET [Dempster et al., 2020], MiniROCKET [Dempster et al., 2021], MrSQM
132 [Nguyen and Ifrim, 2021, 2022] and FreshPrince [Middlehurst and Bagnall, 2022], were tested.
133 Lastly, *ensemble methods* were applied, aiming to mix together time series and tabular models, to
134 combine their predictions and strengths. Nonetheless, these approaches have been outperformed

Table 1: Accuracy results, evaluated on the 3-fold cross-validation, for the tabular methods considered, coupled with feature selection strategies.

Method	Accuracy
Ridge Classifier	0.760
LDA	0.747
Feature Selection + Ridge Classifier	0.777
Feature Selection + LDA	0.778
No water + Ridge Classifier	0.777
No water + LDA	0.783
Feature Selection + Polynomial Features + LDA	0.844
No water + Feature Selection + Polynomial Features + LDA	0.844

Table 2: Examples of *RPolyTransformer* features used. Here x_j denote the j -th wavelength.

$$\begin{aligned}
 &(x_{32} * x_{19}) + x_{103} - x_2 \\
 &(x_{102} * (x_{78}) + x_{26}) \\
 &(x_1 - x_{150}) + x_{64} * x_4 * x_5
 \end{aligned}$$

135 by the ones mentioned above, therefore the corresponding results are not shown in the next
 136 sections.

137 3.1.1 Tabular models, feature selection and transformation

138 In Table 1, results for the best tabular methods are presented. Both the ridge classifier, appro-
 139 priately tuned, and LDA performed quite well, while being extremely fast to train. Nonetheless,
 140 the selection of some specific wavelengths seemed to improve the accuracy further. In fact, both
 141 the removal of the noisy water regions and the data-driven feature selection (performed using
 142 the `SelectFromModel` routine in Python), provides better results.

143 Nevertheless, all these approaches hover around 80% accuracy, therefore, in order to improve
 144 it, the data were augmented considering polynomial features of degree two (using `sklearn`
 145 method `PolynomialFeatures(degree = 2)`). This led to an increase of the accuracy to 84.4%.
 146 The LDA component visualisation for the model with Feature Selection and Polynomial Features,
 147 applied on the unlabeled test dataset, is shown in Figure 1 and a good discrimination between
 148 the three classes is clearly visible.

149 The improvements obtained when considering polynomial features, come at a price in terms
 150 of the computational requirements. In fact, starting from the 1060 original wavelengths, the
 151 addition of second-degree polynomial features resulted in a total number of variables which
 152 made the model estimation task unfeasible. To address this issue, in this work a new *Random*
 153 *Polynomial Features* (`RPolyTransformer` in the following) approach was introduced. The key
 154 idea was to implement random sampling in the non-linear feature space. This lead to relevant
 155 advantages as the total number of features can be controlled and it can consider both higher-
 156 degree (> 2) polynomial features and complex mathematical functions (e.g., cosine, exp).

157 This strategy firstly generated K random arithmetic expressions (see Table 2 for some ex-
 158 amples), which are then used to compute K non-linear features. From the new and the original
 159 features, K^* variables are selected using `SelectKBest` from `sklearn`. The hyperparameters K
 160 and K^* were optimized via cross-validation in the final model (see the final row of Table 3).

161 In Table 3 the results obtained with this method, again combined with different classifiers and
 162 feature selection approaches and tested with the full data and the data after water region removal,
 163 are presented. At first, when combining `RpolyTransformer` with a classifier, a significant drop
 164 in the accuracy was observed, if compared with simple tabular models. Ridge was more accurate
 165 than LDA but it was still far behind the previous results. However, by carefully filtering the



Figure 1: LDA visualisation for the model *Feature Selection + Polynomial Features + LDA*, applied to the unlabeled test data to predict class labels.

166 features either automatically with `SelectFromModel` or manually by removing the water regions,
 167 the results improved noticeably. In these experiments, LDA outperforms Ridge consistently.
 168 Compared to the `PolynomialFeatures` method, the one proposed here is faster (a few seconds
 169 versus a few minutes) and just as accurate. However, the initial results without noise reduction
 170 (i.e., feature selection) suggest that this strategy is more sensitive to noise in the data.

171 3.1.2 Deep Learning Models

172 When considering deep learning models, the task of exploring the feature space and learning
 173 feature interactions is completely deferred to the network, without requiring any feature engi-
 174 neering steps. In turn, deep neural networks require a careful design process, to avoid overfitting
 175 and to identify the best model architecture and input modality.

176 The designed model architectures considered here can be grouped into two main categories,
 177 namely, Fully Connected Networks (FCNs) and Convolutional Neural Networks (CNNs). FCNs
 178 do not require any manipulation or adaptation of the input data, as each single wavelength
 179 is treated as an independent feature and fed to an input unit. In contrast, CNNs require the
 180 data to be bi-dimensional, image-like matrices, as they are commonly used to address image
 181 classification problems. For this family of networks, the input waves need then to be vertically
 182 stacked as 2D arrays and therefore, in order to fit the closest squared dimension, padded with
 183 trailing zeros. An example of how the spectroscopy samples can be presented to the CNNs is
 184 provided in Figure 2. Additionally, a third group of models is tested for this challenge, namely,
 185 CNNs based on dilated kernels (further denoted as `CNN_DILATED`). Whilst regular CNNs
 186 extract features through compact squared filters, or local receptive fields, the `CNN_DILATED`
 187 network utilizes filters that are spatially dilated by a fixed factor [Yu and Koltun, 2015]. Dilated
 188 kernels are commonly used in semantic image segmentation.

189 All the models in this group were trained on both the full training dataset and on the water
 190 reduced one. When the CNN models were trained, the full data were shaped into images of
 191 shape 33×33 with a padding of 29 values, while the reduced data were shaped into images of
 192 shape 23×23 with a padding of 11 values. As already mentioned, all padding values were zeros,
 193 and they were appended to the original sequences.

194 The full list of the implemented architectures is presented in Table S1 in Appendix A.1. The

Table 3: Results for different combinations with *RPolyTransformer*. *SelectFromModel* and *SelectKBest* are feature selection modules to remove noise from data (the former) and select the most discriminative non-linear features (the latter).

Method	Accuracy
Region: FULL	
RPolyTransformer + Ridge Classifier	0.717
RPolyTransformer + LDA	0.619
SelectFromModel + RPolyTransformer + SelectKBest + LDA	0.848
Region: [925:1585, 1720:2989]	
RPolyTransformer + Ridge Classifier	0.805
RPolyTransformer + LDA	0.847
SelectFromModel + RPolyTransformer + SelectKBest + LDA	0.843
Region: [925:1585, 1720:2989, 3738:3807]	
RPolyTransformer + Ridge Classifier	0.811
RPolyTransformer + LDA	0.833
SelectFromModel + RPolyTransformer + SelectKBest + LDA	0.835
Optimized model	
Region: [925:1585, 1720:2989]	
RPolyTransformer($K = 17000$) + SelectKBest($K^* = 7000$) + LDA	0.864

Table 4: Training results on the 3CV splits.

Model	Data	Split 1	Split 2	Split 3	Average
FCN	FULL	0.670	0.677	0.675	0.674
	NO WATER	0.854	0.851	0.837	0.847
CNN	FULL	0.686	0.684	0.670	0.680
	NO WATER	0.806	0.836	0.832	0.824
CNN_DILATED	FULL	0.678	0.684	0.652	0.671
	NO WATER	0.824	0.812	0.807	0.814

195 experiments were conducted on the previously described 3-fold cross-validation splits; note that,
196 for each split, 20% of the training data was held back for validation purposes, to identify network
197 hyperparameters such as number of training epochs, initial learning rate, or regularisation rates.
198 Models were trained for a total of 50,000 epochs, with an early stopping policy used to monitor
199 the validation loss to detect overfitting and save time during the training phase. The final
200 model used to classify the provided unknown data was selected as the overall best performing
201 architecture, and trained over the full training data for a number of epochs set as the average
202 of the epochs reached during the 3CV training.

203 All models were implemented using TensorFlow [Abadi et al., 2016], and trained on a work-
204 station featuring a single GPU, model Nvidia Titan XP. Results are presented in Table 4, which
205 contains the training performances obtained over the 3-folds CV experimental campaign. For
206 all the tested architectures, excluding the water regions from the input waves resulted in a
207 performance increase of roughly 12-13%. The FCN model working on data after water-region
208 removal, achieved the highest accuracy across the 3 splits, with an average of 84.7%. Simi-
209 lar unreported results were obtained also considering a single split validation strategy, which
210 furthermore demonstrated that convolutional models tend to overfit the input data quite fast.

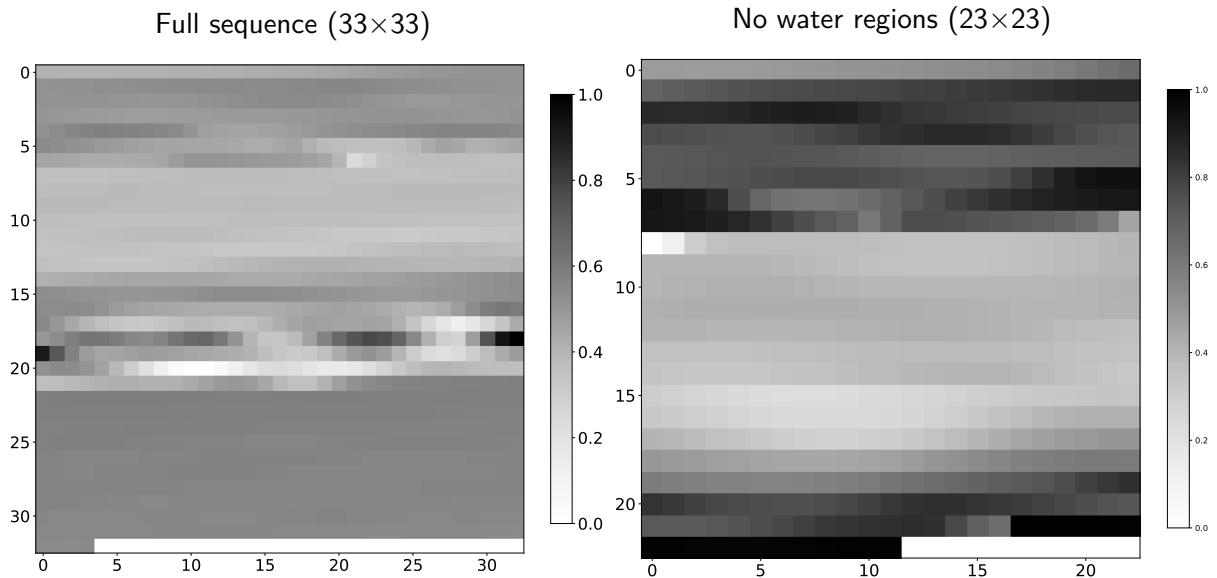


Figure 2: Spectroscopy sequences arranged as image structures. In both examples, the padding values are visible at the bottom of the resulting images. Values are normalised in the 0-1 range for convenience.

Table 5: Confusion matrix obtained by combining LDA and SVM.

		Predicted class		
		CLV	GRS	TMR
True class	CLV	83.5%	17.4%	0.7%
	GRS	15.8%	81.6%	0.8%
	TMR	0.7%	1.1%	98.5%

211 3.2 Participant 2

212 All the processing steps and the algorithm implementation was completed using MATLAB [MAT-
 213 LAB, 2018]. After having imported the dataset in tabular form, the outliers were identified as
 214 those observations with at least one wavelength with more than three scaled median absolute
 215 deviation from the wavelength specific median (see [https://uk.mathworks.com/help/matlab/
 216 ref/isoutlier.html](https://uk.mathworks.com/help/matlab/ref/isoutlier.html) for further details). Classification was performed using a set of algorithms
 217 such as Support Vector Machine (SVM), K-Nearest Neighbors (KNN) and Linear Discriminant
 218 Analysis (LDA). To optimize the number of predicting variables, coefficient's threshold and the
 219 regularization parameter was tuned using a 5-fold cross-validation and classification accuracy
 220 was evaluated.

221 The best results were obtained using LDA, which was able to distinguish outdoor grass-feed
 222 cow's milk from TMR with an accuracy of 95% while differentiating grass and clover with an
 223 accuracy of 68%. Figure 3 allows to visualize class boundaries by plotting the spectra projections
 224 in the latent space spanned by the two discriminant functions. From the figure, a clear boundary
 225 can be observed between the indoor and outdoor feed classes, while there is a significant overlap
 226 between the GRS and CLV classes. Therefore, the extracted components were then considered
 227 as an input to a linear SVM model to improve classification between outdoor feed classes. The
 228 combination of two classifier (LDA + SVM), resulting in a two-step approach, significantly
 229 improved the overall classification accuracy (87.1%) as well as classification accuracy between
 230 classes, as shown in Table 5.

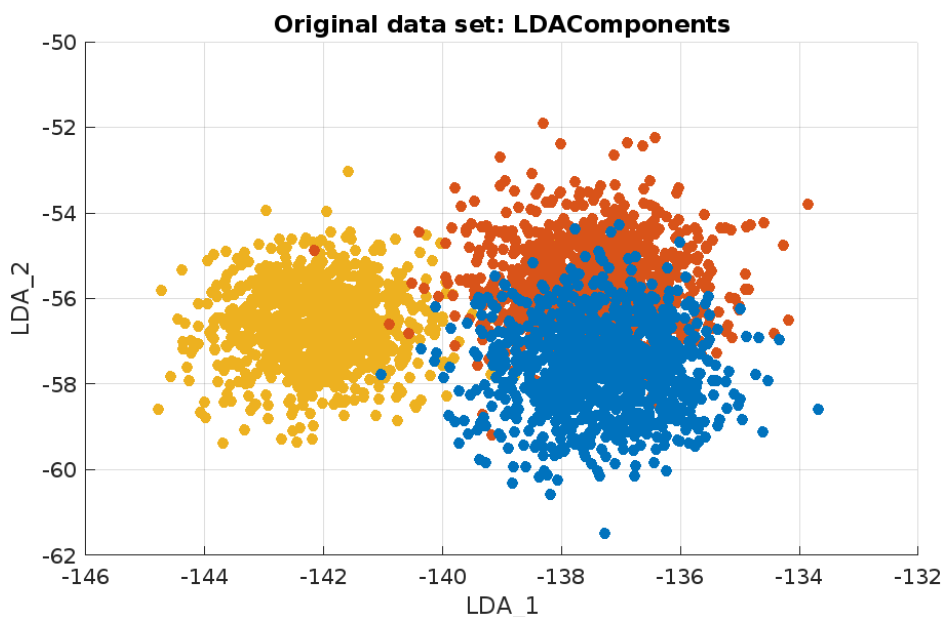


Figure 3: LDA components extracted from the developed model.

231 3.3 Participant 3

232 The present work was developed independently by three group members, following a common
 233 preliminary analysis of spectral data. Results of the prediction on the test set provided for the
 234 chemometric challenge were then compared to assess the agreement between the three different
 235 statistical approaches employed.

236 3.3.1 Preliminary edits on spectral data

237 These edits were conducted on raw spectral data in both the training and test sets using Python.
 238 Spectra expressed in transmittance were converted into absorbance by taking the \log_{10} of the
 239 reciprocal of the transmittance. Subsequently, spectral wavelengths associated to water ab-
 240 sorption, as well as non-informative regions, were deleted. This led to a reduced version of
 241 the dataset, that has been used for the subsequent analyses, with 511 remaining wavelengths
 242 in the regions between 2,994 and 1,682 cm^{-1} and between 1,578 and 926 cm^{-1} . A graphical
 243 representation of this procedure is reported in the supplementary material (Figure S1).

244 3.3.2 First approach

245 To explore the multivariate structure of the dataset, Principal Component Analysis (PCA) was
 246 exploited on the training dataset, using `prcomp` function in `stats` package and the `factoextra`
 247 package [Kassambara and Mundt, 2020] in the R environment R Core Team [2020]. The analysis
 248 revealed that most of the data variability was explained by the first two Principal Components
 249 (PCs), accounting together for the 88% of the total variance (see the scree plot on the left top
 250 panel in Figure 4).

251 Afterwards, possible outliers were detected using the algorithm proposed by Filzmoser et al.
 252 [2008] and implemented in the `mvoutlier` package [Filzmoser and Gschwandtner, 2021]; only the
 253 observations being both location and scatter outliers were removed from the training dataset.
 254 As a results, a total of 63 observations were removed from the training dataset.

255 After outliers removal, linear discriminant analysis was considered using `lda` function in the
 256 MASS package [Venables and Ripley, 2002]. To test its accuracy, as a first step the discrimi-
 257 nant functions were applied to the training dataset, with the aim of comparing the estimated
 258 classification with the actual one. Therefore, LDA was first applied to maximize the differences

Table 6: Summary of the results of the three different approaches.

	Approach 1	Approach 2	Approach 3
Brief description	Two steps DA in R	Canonical DA with stepwise method in SAS	DA with stepwise methods in SPSS
Number of samples (training set)	3180	3116	3153
Number of wavelengths retained	511	88	16
Accuracy (training set)	83.30%	81.32%	71%
Predicted diet for the samples in the test dataset (n cases)			
TMR	344	326	365
CLV	367	342	326
GRS	366	353	386
Agreement between the approaches applied to the test dataset			
Member 1			
Member 2	84.21%		
Member 3	72.90%	70.84%	

259 between TMR and the CLV+GRS (in the following named PAST group). The LDA returned
260 one Linear Discriminant (LD) function, which was then applied to the training dataset to at-
261 tribute the TMR diet to observations. Afterwards, LDA was applied again by maintaining in
262 the training set only the observations belonging to the PAST group. The obtained LD function
263 was then applied to the whole training dataset to discriminate between CLV and GRS diets
264 previously categorized as PAST. The vector with the predicted classes was then compared with
265 the vector of actual group classification in the training dataset, thus computing the training
266 accuracy. This approach resulted in an overall model training accuracy equal to 83.3% (see
267 Table 6); the scatter plot of the first versus second linear dimension scores is depicted in the
268 right top panel in Figure 4. Lastly, the LD functions obtained on the training dataset allowed
269 for the classification of the unknown observations in the test dataset, with the results reported
270 in Table 6.

271 3.3.3 Second approach

272 Principal component analysis (PROC PRINCOMP, SAS Institute Inc., ver. 9.4) was undertaken
273 on the training set, as in Section 3.3.2. Coherently, outlier removal was then performed by
274 calculating the Mahalanobis distance (MD) as the uncorrected sum of squares of the first four
275 centred and scaled PC scores, explaining up to the 98.21% of the total spectral variance. Outliers
276 were defined as samples whose MD was greater than the 97.5th percentile of a χ^2 distribution
277 with 4 degrees of freedom [Brereton, 2015]. Following this approach, a total of 127 samples were
278 discarded from the training set.

279 The discriminant model was developed following a multiple-step approach. Firstly, a step-
280 wise discriminant analysis was carried out in order to identify the most significant wavelengths
281 associated with the three different diets using the PROC STEPDISC. A total of 88 wavelengths
282 were retained and used for the subsequent canonical discriminant analysis, which was developed
283 through the PROC DISCRIM. The proportion of samples correctly classified was 73.38% (CLV),
284 73.70% (GRS), and 97.62% (TMR), with an overall model accuracy of 81.32%. The scatter plot
285 of the first versus second canonical variables scores is in the bottom left panel of Figure 4. The
286 wavenumbers with the greatest (in absolute value) canonical discriminant function coefficients
287 were between 1,154 and 1,162 cm^{-1} , 2,843 cm^{-1} , 2,874 cm^{-1} , and 2,882 cm^{-1} , thus providing
288 some potentially relevant information to be explored to assess which milk chemical features are

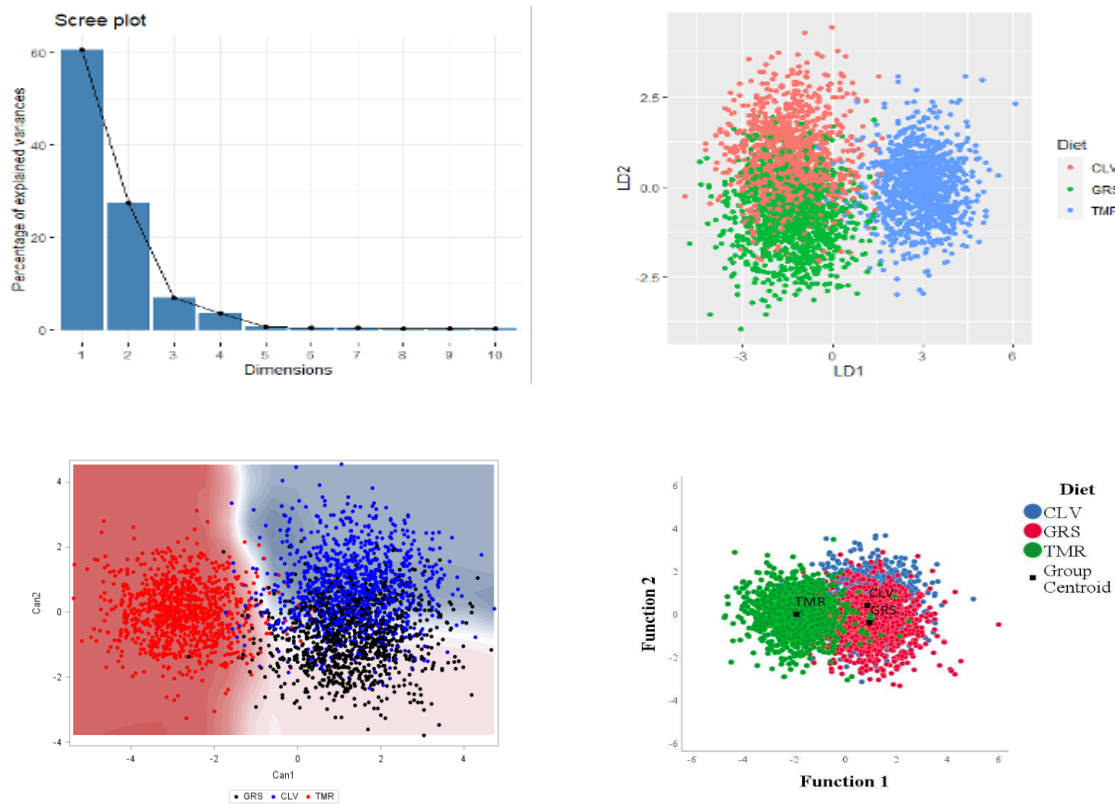


Figure 4: Explained variance by the first 10 principal components (top left), scatter plot of discriminant models developed by member 1 (right top), member 2 (bottom left) and member 3 (bottom right).

289 more influenced by the dietary regimen. The discriminant model was then applied to the test
 290 set to obtain the prediction of cows' diet on unknown milk spectra.

291 3.3.4 Third approach

292 Standard assumptions required for multivariate analyses were verified before proceeding to the
 293 main analysis. Two diagnostic measures were used to identify the outliers for the predictors
 294 and the dependent variables; in the former case Mahalanobis Distance (MD) was used to spot
 295 multivariate outliers while, in the latter one, studentized residuals were considered. Samples
 296 whose MD was greater than the 97.5th percentile of the MD distribution and studentized
 297 residuals greater than 2.5 were removed. During this process, a total of 90 outliers have been
 298 identified and excluded. Potential multicollinearity was then verified by Tolerance and Variance
 299 Inflation Factors. Moreover, the ratio between the number of cases and predictors was checked
 300 as an indicator of the adequacy of the sample size; a ratio of 20 observations for each predictor
 301 variable, with the smallest group size exceeding the number of independent variables, is suggested
 302 [Meloun and Militký, 2011; Pituch and Stevens, 2015].

303 LDA was then chosen as the main discriminative approach. The stepwise method, using
 304 Wilks' lambda Λ as criterion, was adopted to reduce multicollinearity and increase the
 305 case/predictors ratio, improving the adequacy of the sample size. Box's test and log determi-
 306 nants were considered to verify the equality of covariance matrices. The canonical correlation
 307 and the proportion of between-group variance that is due to each variate were used as mea-
 308 sures of effect size [Pituch and Stevens, 2015], while the performance of the LDA was evaluated
 309 by classification-related statistics and leave-one-out CV [Hahs-Vaughn, 2016]. The **Scoring**
 310 **Wizard** command was finally used to apply the discriminant functions (DF) to the test dataset,

311 and the predicted probability was calculated to assess its performance. Analyses were performed
312 with SPSS software [IBM Corp., 2017].

313 Standardized canonical DF coefficients of the variables selected by DA and measures of effect
314 size are shown in Table S2 in the Supplementary Material. More than 90% of the total difference
315 between the groups was attributable to the first DF, with the Wilks' Λ (0.330) indicating that it
316 has a significant discriminating capacity (p-value < 0.001). Wavenumber 2,851 cm^{-1} and 2,890
317 cm^{-1} mostly contributed to the discrimination of cows' diet. The second DF only explained
318 6% of the total variance, being nonetheless still significant (Wilks' Λ = 0.902; p-value < 0.001).
319 Centroids (Table S3) and the plot of DF scores (bottom right panel in Figure 4) indicated
320 that the first DF appropriately discriminate the TMR group from the others (i.e., CLV and
321 GRS). On the other hand, group separation on the second DF was poor; in particular, CLV and
322 GRS clusters were not clearly distinguished. The cross-validation procedure indicated an overall
323 model accuracy of 71% (see Table 6), with different sensitivity between groups: over 90% for
324 TMR samples, and below 65% for CLV and GRS samples. The application of DFs to predict
325 the diet of cows in the test data set showed a similar trend, with an expected sensitivity of 64%,
326 63%, and 87% for CLV, GRS, and TMR diets, respectively (Table S4).

327 Lastly note that, all the three approaches were applied and the results were compared at the
328 end of the competition. Despite the better prediction performance shown by the first approach
329 on the training set, the second approach proved to be the best for the prediction of the test set.

330 3.4 Participant 4

331 A conventional machine learning pipeline was used, composed of feature (i.e., wavelength) selec-
332 tion and classification, with no outliers being removed from the original dataset. Dimensionality
333 reduction techniques such as Principal Component Analysis (PCA) and Independent Compo-
334 nent Analysis (ICA), as well as Extended Multiplicative Scatter Correction (EMSC) and a data
335 augmentation approach were tested to improve the classification results [Bjerrum et al., 2017].
336 EMSC represents a preprocessing technique which removes multiplicative effects potentially
337 caused by physical phenomena such as light scattering, which is commonly seen in reflectance
338 spectroscopy, thus allowing for easier modelization of chemical effects. On the other hand, the
339 data augmentation scheme increases the data set ten fold by adding random variations in offset,
340 multiplication, and slope, nine times to each sample. The variations were ± 0.1 times the stan-
341 dard deviation of the training set for the offset, multiplication was 1 ± 0.1 times the standard
342 deviations, and the slope adjustment was between 0.95 and 1.05 [Bjerrum et al., 2017].

343 Subsequently a range of different classifiers, which have successfully been adopted before
344 on infrared spectroscopy data, were used. In particular, the considered models were K-nearest
345 Neighbour [K-NN; Balabin and Safieva, 2011], Random Forest [RF; Chen et al., 2021], Sup-
346 port Vector Classification [SVC; Ji-yong et al., 2013], Multilayer-perceptron [MLP; Balabin and
347 Safieva, 2008], Linear Discriminant Analysis [LDA; Khuwjitjaru et al., 2020], Decision Tree
348 Classification [Geronimo et al., 2019], Nu-Support Vector Classification [NuSVC; Terouzi et al.,
349 2013], AdaBoost Classification [Wu et al., 2017], Gradient Boosting Classification [Munera et al.,
350 2021], Gaussian Naive Bayes [Bhati and Bhattacharya, 2020] and Quadratic Discriminant Anal-
351 ysis [QDA; Oravec et al., 2019]. Other investigated predictive methods belonged to the group of
352 deep Learning (DL) techniques, and in particular one-dimensional (1D) Convolutional Neural
353 Network (CNN). This 1D CNN makes use of six one dimensional convolutional layers, and a
354 number of max pooling, batch normalization and dropout layers. Each 1D CNN layer is followed
355 by a max-pooling and batch normalization layer. The one-dimensional CNN only used the raw
356 spectra, as the use of PCA and FastICA would be detrimental due to the transformation of the
357 sequence of the data.

358 Prior to the analyses, the dataset was split into a training set (80% of the data), to train
359 different models, and a validation set (remaining 20% of the data), used to optimise the hyper-
360 parameters and to identify the best methods to be used for the final testing. This split was

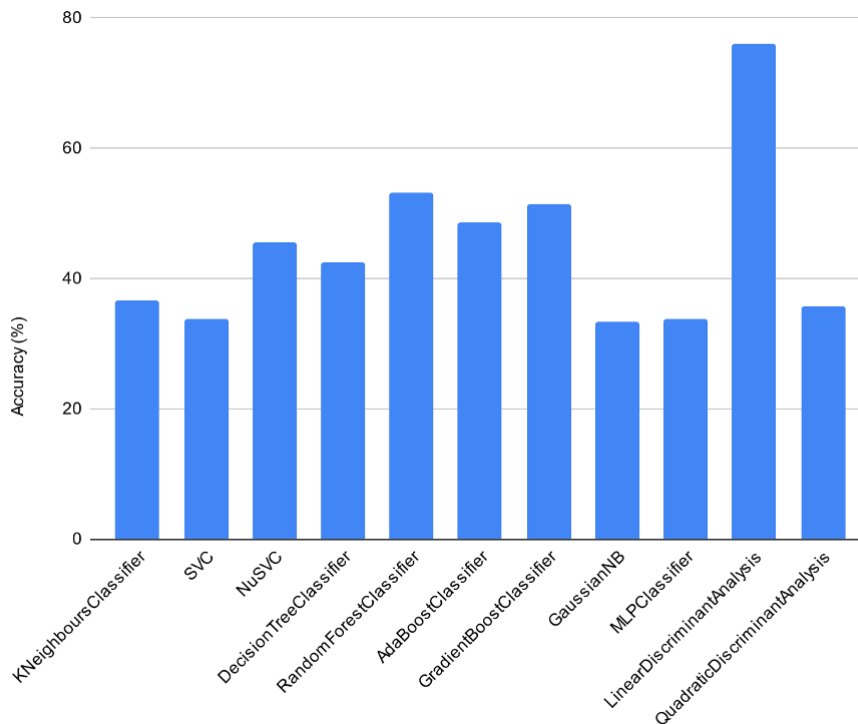


Figure 5: Results of classifiers on a 80/20 test-train split.

361 made by utilizing the `train_test_split` function provided through `scikit-learn` [Pedregosa
 362 et al., 2011].

363 An initial experiment was performed on all classifiers without the use of data augmentation
 364 or feature selection. This was carried out to explore which classification method was performing
 365 better with the raw spectral data. Figure 5 shows the results obtained from the initial step
 366 with the 80/20 train/validation for different classifiers. All results gathered were averages taken
 367 from three training and validation predictions for each model. LDA gave the best results with
 368 an accuracy of 76%, whereas the MLP and SVC produce some of the worst performances with
 369 accuracies around 33%.

370 In the second stage, the classifiers were tested in conjunction with PCA, ICA or data aug-
 371 mentation: for PCA and FastICA `scikit-learn` methods were used, with the parameters being
 372 setted as `FastICA(tol = 0.02, max_iter = 4000)` and `PCA(n_components = 800)`. The use
 373 of PCA and ICA altered the data by reducing the dimensionality, while on the other hand
 374 data augmentation increased the number of samples. For data augmentation, the data augment
 375 function from Bjerrum et al. [2017] was used. This increased the number of training samples
 376 from 3,244 to 19,464. At this stage, only a subset of the previously tested model were con-
 377 sidered, based on their performances in the previous step. Figure 6 shows the results of each
 378 classifier with each pre-processing method (base, ICA, PCA, data augmentation (Aug)). From
 379 these results, it was noted that LDA following data augmentation achieved the highest accuracy
 380 with 82.7%. The greatest improvement in the predictions was observed using MLP after ICA
 381 (improvement of 41%). An additional experiment was then carried out with just the use of the
 382 LDA model. This was to show the importance of regions within the spectra, and a number of
 383 different wavelength region were tested. Therefore, figure 7 shows the results of the LDA when
 384 removing different spectral regions.

385 There was a general increase in accuracy over the base approach when data augmentation
 386 was used, with the only exception of CNN. With regard to wavelengths selection, there was no

Base, ICA, PCA and Aug

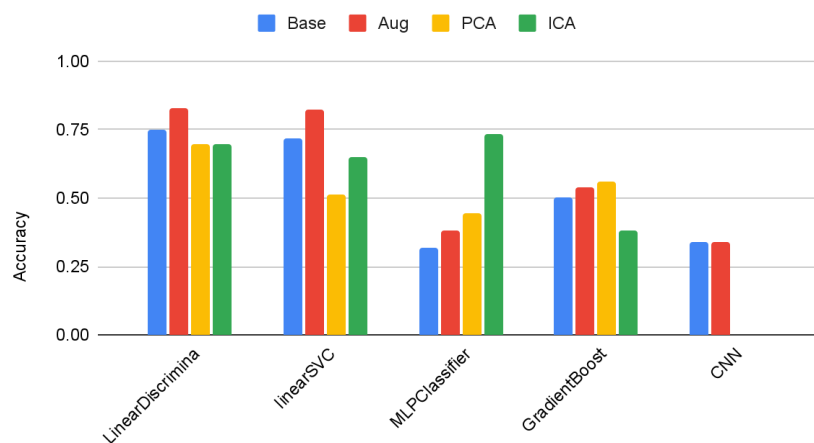


Figure 6: Results of classifiers on with different pre-processing methods.

Range of Spectra With LinearDA

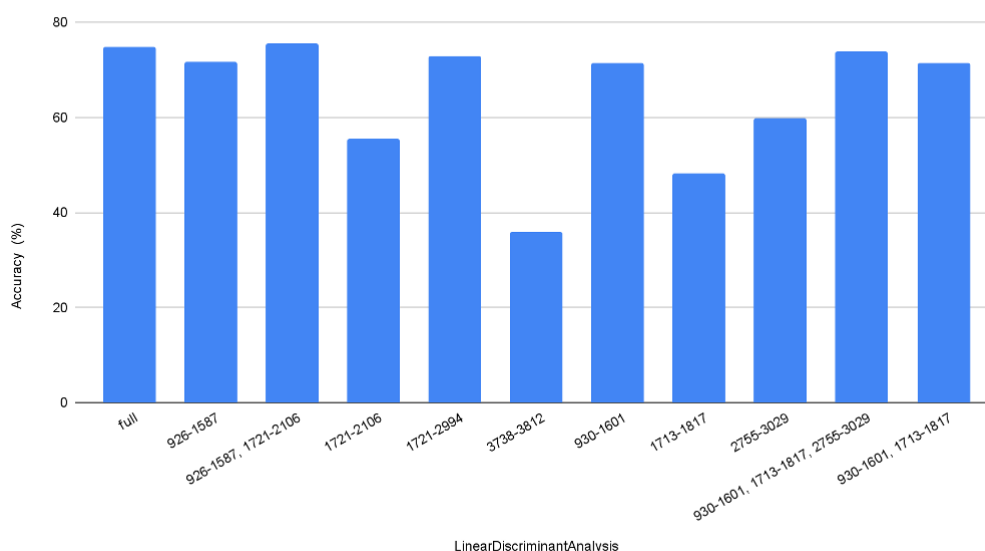


Figure 7: Results of Linear Discriminant Analysis for different feature selection.

387 noticeable increase in accuracy when focusing on a specific region in the spectra. Nonetheless,
 388 the majority of the relevant information lied within the region from 925 cm^{-1} and 1597 cm^{-1} ,
 389 and there was a slight increase in the accuracy of prediction of around 1% when using the range
 390 of 925 to 1585 cm^{-1} and 1717 to 2103 cm^{-1} compared to the full set of wavelengths.

391 3.5 Participant 5

392 In order to prepare the data set for predictive analysis, some pre-processing was considered.
 393 As directed by the challenge organisers, outlying spectra were removed such that the data set
 394 consisted of 3243 transmittance spectra covering 1060 wavelengths. Spectra were transformed
 395 to absorbance values by taking \log_{10} of the reciprocal of the transmittance values. In addition,
 396 following Frizzarin et al. [2021b], a subset of 534 wavelengths that lay outside the water-related

397 high-noise-level regions were identified as relevant for predicting a cow’s diet, although the
 398 water-regions were not excluded at this point in the analysis.

399 To ensure a robust assessment, the dataset was split into training and validation sets. In this
 400 case, the validation set was constructed to control for batch effect confounding, which may bias
 401 estimates for out-of-sample prediction [Soneson et al., 2014]. Inspection of the data set revealed
 402 that rows were ordered to have several consecutive observations of each diet. Therefore, it
 403 was assumed that each set of consecutive diet observations belonged to a single batch. In this
 404 manner, 90 batches, 30 for each diet, were identified. In addition, the data was collected over
 405 three years [Frizzarin et al., 2021b], and so it was assumed that the first 30 batches were collected
 406 in the first year of the study, the next 30 in the second year, and the final 30 in the third. Based
 407 on these assumptions, the validation set consisted of 996 spectra from 30 batches collected in
 408 the study’s third year, which included ten batches for each diet, while models have been trained
 409 on the 2247 remaining spectra. Training data was randomly split into $V = 10$ folds, with each
 410 fold including two batches from each diet. Possible batch effect of repeated measurements for a
 411 single cow were ignored.

412 In order to describe the predictive model used in this analysis, let $\mathcal{D} = \{y_i, \mathbf{x}_i\}_{i=1}^N$ denote the
 413 observed data, where the response variable $y_i \in \{1, \dots, M\}$ represents the diet of the i -th cow
 414 and covariates $\mathbf{x}_i \in \mathbb{R}^D$ represent the corresponding milk absorbance spectrum. Note that this
 415 analysis considers $M = 3$ diets, $D = 1060$ wavelengths, and $N = 3243$ training observations.
 416 The objective of the proposed predictive models is to learn $\mathbb{P}(y | \mathbf{x})$, that is, the probability that
 417 a given milk sample comes from a grass, clover or TMR-fed cow, given the spectrum for that
 418 sample.

419 The first step in constructing a predictive model is to define a deterministic mapping function
 420 $g : \mathbf{x}_i \rightarrow \mathbf{z}_i$, for $\mathbf{z}_i \in \mathbb{R}^{D'}$, with $D' < D$, which describes a feature extraction procedure. Two
 421 approaches to feature extraction were considered here. The first simply selected the $D' = 534$
 422 relevant wavelengths identified by Frizzarin et al. [2021b] such that \mathbf{z}_i is the i -th absorbance
 423 spectrum after removing the high-noise-level water regions and standardises each wavelength.
 424 The second was based on the wavelet transform, a popular technique for signal processing which
 425 can be applied for data compression, smoothing, and multi-resolution analysis [Nason, 2008], and
 426 proceeds in three steps. After setting high-noise-level regions of each spectrum to 0, a thresholded
 427 wavelet transform provides a set of wavelet coefficients. The feature vector \mathbf{z}_i is then the vector
 428 of wavelet coefficients that are non-zero for at least one of the N spectra, in this case $D' = 594$.
 429 The thresholded wavelet transform is available with the `wavethresh` R package [Nason, 2016],
 430 using Daubechies least symmetric wavelet as the mother wavelet and Bayesian approach to
 431 thresholding wavelet coefficients [Abramovich et al., 1998]. Note that setting wavelengths in
 432 the high-noise-level regions to 0 means the wavelet transform preserves the spectral distance
 433 between wavelengths while ensuring that the corresponding wavelet coefficients are 0.

434 Given the feature vector $\mathbf{z}_i = g(\mathbf{x}_i)$, a multinomial regression model for diet was assumed,
 435 such that

$$\mathbb{P}(y_i = m | \mathbf{z}_i) = \frac{\exp(\beta_m^\top \mathbf{z}_i)}{\sum_{l=1}^M \exp(\beta_l^\top \mathbf{z}_i)}, \quad (1)$$

436 for $m = 1, \dots, M$ where $\beta_m \in \mathbb{R}^{D'}$, implicitly assuming that \mathbf{z}_i includes an intercept term.
 437 The `glmnet` package [Friedman et al., 2010] fits this model to data efficiently. For simplicity, a
 438 LASSO model was fitted, where 10-fold cross-validation on the training data informs the penalty
 439 hyperparameter.

440 Finally, the predictive performance of the proposed models was compared by analysing their
 441 log-loss on the validation data set. That is, for a validation data set and a model \mathcal{M}_j for
 442 $\mathbf{z}_i = g(\mathbf{x}_i)$, the log-loss is defined as

$$\ell_j = -\frac{1}{N'} \sum_{i=1}^{N'} \sum_{m=1}^M \mathbb{I}(y_i = m) \ln \mathbb{P}(y_i = m | \mathbf{z}_i, \mathcal{M}_j), \quad (2)$$

Table 7: Predictive model assessment.

Model	In-sample log-loss	Validation log-loss
Raw Spectra	0.57	0.82
Wavelet Coefficients	0.74	0.88

443 where N' is the number of observations in the validation set, $\mathbb{I}(\mathcal{A})$ is the usual indicator function
444 that is equal to 1 when \mathcal{A} is true and 0 otherwise and $\mathbb{P}(y_i = m \mid \mathbf{z}_i, \mathcal{M}_j)$ is the probability under
445 \mathcal{M}_j that $y_i = m$ given \mathbf{z}_i . The log-loss is a proper scoring rule for evaluating predictive models
446 [Gneiting and Raftery, 2007], where smaller scores are better, and so encourages the analysts
447 to express their true belief about the data. It is also straightforward to set benchmarks for
448 assessing the quality of predictions a priori. For example, for any M a mean log loss of 0
449 represents perfect predictive performance, while when $M = 3$ as in the considered case, a mean
450 log loss of $-\ln(1/3) \approx 1.1$ represents “guessing”, where we predict each category uniformly at
451 random. For completeness, the classification accuracy of \mathcal{M}_j was also assessed.

452 The results of this analysis are presented in Table 7. The first model considered was a LASSO-
453 penalized multinomial regression of the raw milk spectra on the diet, where high-noise-level
454 regions of the spectrum was excluded and the wavelengths standardised. The tuning parameter
455 λ , controlling the strength of the penalization, was selected to minimise the multinomial deviance
456 (a statistic proportional to the mean log-loss) via 10-fold cross-validation. The log-loss of this
457 model on the training set was 0.57, which corresponds to a diet classification accuracy of 77%.
458 A closer examination of the predictions revealed that when CLV and GRS were treated as a single
459 category (pasture-fed), it was possible to predict TMR with an accuracy of 94%. When trying
460 to predict whether the cow was fed CLV, given that it was pasture-fed, an accuracy of 72% was
461 achieved. Predictive performance was much poorer on the validation set, with an overall log-loss
462 of 0.82, corresponding to an accuracy of 58%. The model predicted TMR with an accuracy of
463 88%. However, for cows known to be pasture-fed, it predicted CLV with an accuracy of 49%.

464 The second model considered a multinomial regression of the non-zero thresholded wavelet
465 transform coefficients of the milk spectra on diet. As above, the model was fitted by maximising
466 a penalised log-likelihood and by using 10-fold cross-validation to tune λ . For this model, the
467 log-loss on the training set was equal to 0.74, corresponding to an accuracy of 69%, although it
468 predicted TMR with an accuracy of 88%. For pasture-fed cows, it predicted CLV with an accuracy
469 of 68%. As with the first model, performance dropped for the validation set. The log-loss was
470 0.88 and TMR accuracy was 79%. Given that a cow was pasture-fed, the CLV accuracy was 47%.
471 These results are summarised in Table 7.

472 The obtained results clearly showed that milk spectra carry a signal distinguishing pasture-
473 fed cows from TMR, but that it was difficult to distinguish between CLV and GRS. However, the
474 predictive performance was much poorer on the validation dataset than for the training one,
475 indicating that the adopted models did not offer a robust out-of-sample predictions. Without
476 careful consideration of potential batch effect confounders within the sampled spectra, we are
477 likely to overestimate the out-of-sample performance of our models. Collecting data from more
478 cows over a more extended period should alleviate this issue and allow more robust models to
479 be developed.

480 Lastly, no evidence was found to suggest that wavelet transformed spectra provided helpful
481 insight into the cows’ diet. However, that is not to say that some alternative basis expansion
482 could improve the current predictive models. In fact, given more data on the relationship be-
483 tween milk spectra and diet, the development of models which allow for non-linear relationships
484 between wavelengths may prove a fruitful avenue for future research.

485

486 3.6 Participant 6

487 As a first step, the training set was centered and scaled and the same transformation was
 488 applied to the test set. In the following analyses, no outliers were removed while all the spectra
 489 were transformed from transmittance to absorbance. Wavelengths from high-noise level spectral
 490 regions between 1720 and 1592 cm^{-1} , between 3698 and 2996 cm^{-1} , and greater than 3,818
 491 cm^{-1} were removed from the analysis following Frizzarin et al. [2021b].

The Fisher score, being the ratio of between to within diet group variance, was calculated for all the wavelengths in the training set. For wavelength j , the Fisher score is given by:

$$\text{Fisher score}_j = \frac{\sum_{m=1}^M \sum_{i=1}^n \mathbb{I}(y_i = m) (\bar{x}_{.j}^{(m)} - \bar{x}_{.j})^2}{\sum_{m=1}^M \sum_{i=1}^n \mathbb{I}(y_i = m) (x_{ik} - \bar{x}_{.j}^{(m)})^2}$$

492 where j denotes the wavelength index, $i = 1, \dots, n$ denotes the spectra with n being the number
 493 of spectra in the training set, m denotes the diet group with $M = 3$, $\mathbb{I}(y_i = m)$ is an indicator of
 494 diet group spectra i , $\bar{x}_{.j}$ is the average of wavelength j for all spectra ($i = 1, \dots, n$), $\bar{x}_{.j}^{(m)}$ is the
 495 average of wavelength j in diet group m . A wavelength with the highest Fisher score in each
 496 of the discarded regions was kept in the analysis. Wavelengths with Fisher score lower than
 497 0.002 were removed from further analysis, thus leaving 380 wavelengths. In order to compare
 498 algorithms and carry out further feature selection, the training set was itself randomly split
 499 75/25 into training and testing sets stratified by diet. A genetic algorithm [Holland, 1992],
 500 implemented in library `genalg` [Willighagen and Ballings, 2022] was used as a stochastic search
 501 method to find an optimal subset of input wavelengths for classification. Individuals in the GA
 502 population were represented by binary strings denoting wavelengths to be included or excluded
 503 for prediction. Objective function was set to be the average accuracy from ten cross-validated
 504 fits of linear discriminant analysis (LDA) of the training subset. GA was run for 200 iterations
 505 with population size set at 200. Figure 8 shows the spectra absorbance and the corresponding
 506 Fisher scores, with points denoting the wavelengths selected by the GA.

507 The best configuration from the final GA population had 70 wavelengths included. These
 508 wavelengths were used as inputs to the following classification algorithms:

- 509 • Linear discriminant analysis (LDA), library `MASS` [Venables and Ripley, 2002];
- 510 • Partial least squares discriminant analysis (PLS-DA) [Mevik et al., 2020];
- 511 • Least absolute shrinkage and selection operator [LASSO; Tibshirani, 1996], library `glmnet`
 512 [Friedman et al., 2010];
- 513 • Elastic net [EN; Zou and Hastie, 2005], library `glmnet`;
- 514 • Random Forest [RF; Breiman, 2001], library `ranger` [Wright and Ziegler, 2017];
- 515 • Support vector machines [Vapnik, 1998], library `kernlab` [Karatzoglou et al., 2004];
- 516 • Bayesian kernel projection classifier [BKPC Domijan and Wilson, 2011], library `BKPC`
 517 [Domijan, 2018].

518 All analyses were done using R [R Core Team, 2020], the code is available in the github
 519 repository https://github.com/domijan/KD_Vistamilk2022.

520 The training set was randomly split into ten further training/testing sets of equal size,
 521 stratified on diet. The average accuracy and standard deviation over the ten random splits
 522 for all the classification algorithms are given in Table 8. LDA performed best with average
 523 accuracy of 77.4%. PLS-DA and EN overall accuracy was of 76.9%, 76.5% respectively. The
 524 algorithms were tuned using further cross-validation of the training sets. For BKPC and SVM,
 525 the best results were obtained with a linear kernel. The predictions of the LDA were submitted
 526 to the competition. Moreover, genetic algorithm was able to select a much smaller subset of
 527 wavelengths without loss of classification performance.

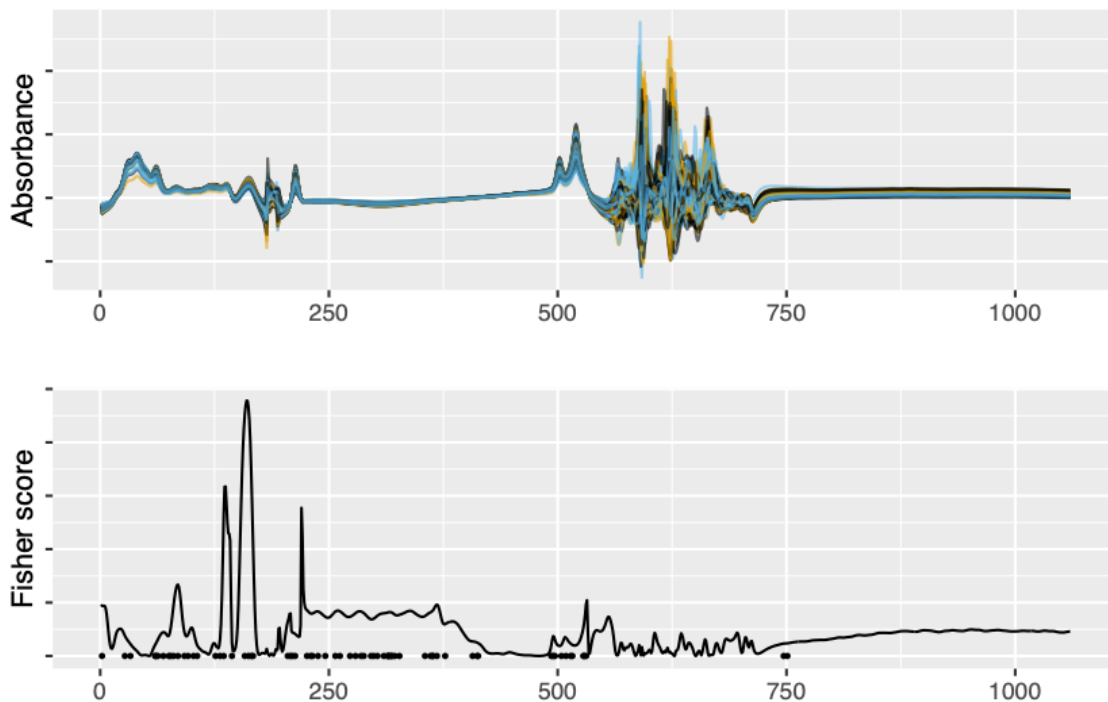


Figure 8: Spectra absorbance and the corresponding Fisher score with points on the x-axis denoting the wavelengths selected by the GA.

Table 8: Average accuracy for over ten random splits of the training set for classifiers. LDA: linear discriminant analysis; PLS: partial least squares regression; EN: elastic net; BKPC: Bayesian kernel projection classifier; SVM: support vector machine; LASSO: Least absolute shrinkage and selection operator; RF: random forest.

Accuracy	LDA	PLS	EN	BKPC	SVM	LASSO	RF
Mean	0.774	0.769	0.765	0.759	0.738	0.736	0.509
SD	0.008	0.009	0.007	0.008	0.007	0.006	0.014

528 4 Discussion

529 While the dataset provided for the data competition included three different classes to dis-
530 criminate (i.e. TRM, GRS, and CLV), the main difficulty of the present data competition was
531 concerned with the discrimination between GRS and CLV diets. In fact, the ability of dis-
532 tinguishing pasture and TMR dietary regimens has been already documented [Frizzarin et al.,
533 2021b], with the discrimination being driven mainly by the different content of fatty acids (FA)
534 in milk [Agradi et al., 2020]. In particular, milk from pasture based diet is generally richer in
535 saturated FA such as linoleic acid, poorer in saturate FA, and have a lower omega6/omega3
536 ratio [see e.g. Chilliard et al., 2007; Dewhurst et al., 2006; Ferlay et al., 2013, 2017]. As MIR is
537 known to be able to predict, with a certain degree of accuracy, the different FA in milk [Soyeurt
538 et al., 2011], spectral data are therefore capable to discriminate also TMR and pasture diets.

539 On the other hand, since GRS and CLV dietary regimens differed only for the inclusion
540 of 20% annual clover in perennial ryegrass sward for the CLV diet, induced differences in the
541 FA might be less clear. As a consequence, to discriminate GRS and CLV exploiting spectral
542 information only, a careful and accurate tuning of the modelling choices was required. In this
543 regard, interestingly, some participants proposed two-steps classification approaches, with the
544 first step focusing on TMR and pasture based diets, while the second one aimed at distinguishing
545 CLV from GRS samples. As an example, participant 2 highlighted a potentially significant gain

Table 9: Accuracy computed on the test dataset for all the participants.

Participant	Sect 3.1.1	Sect 3.1.2	Sect 3.2	Sect 3.3.2	Sect 3.3.3
Test accuracy	0.871	0.837	0.798	0.711	0.783
Participant	Sect 3.3.4	Sect 3.4	Sect 3.5	Sect 3.6	
Test accuracy	0.796	0.786	0.724	0.766	

546 in terms of accuracy when considering an ensemble approach, where components extracted from
547 LDA was used to train a linear SVM, better discriminating between GRS and CLV. Again, in
548 Section 3.3.2 two consecutive LDA models have been fitted, with the first one being used to
549 discriminate TMR from pasture while the second, exploiting the discriminant function on the
550 pasture samples only, was trained to classify GRS and CLV.

551 Generally speaking, linear approaches introduce a gain in interpretability of the results,
552 while paying a price in terms of accuracy. Nonetheless, the review of the different approaches
553 presented in this paper showed that strong performances were achieved resorting to linear clas-
554 sifiers. In fact, remarkable results were obtained when adopting LDA-based approaches (see,
555 e.g., participants 1, 2, 4 and 6), which were certainly proven effective in discriminating TMR
556 and pasture diets and, as highlighted above, were also used as a building block for promising
557 two-steps procedures. Nevertheless, the approaches presented in Sections 3.1.1 and 3.1.2, which
558 attained the best test set prediction accuracies as it is displayed in Table 9, pointed towards the
559 need of considering non-linearities, especially when the aim is to discriminate between GRS and
560 CLV. This is confirmed by the confusion matrix displayed in Table 10, where it is shown that
561 these two different dietary regimens are discriminated remarkably well, especially if considering
562 their similarities from a compositional standpoint. Note that, while with FCN interpretation
563 of the results and exploration of the most informative wavelengths are compromised, the ap-
564 proach in Section 3.1.1, which is considering again LDA as the final classifier, tends to be more
565 transparent. However, the clever random polynomial variables generation proposed tends to
566 produce new features which are difficult to interpret from a chemical standpoint. Therefore, as
567 it often happens in modern data analysis routine, the adopted approaches have to be tailored
568 on the specific aim to pursue, often dealing with the standard trade-off between accuracy and
569 interpretability.

570

571 Data transformations, such as first and second derivative, are extensively used in near in-
572 frared spectroscopy. In the current study with MIRS data, as widely undertaken, the only
573 transformation applied to the spectral data was their conversion from transmittance to ab-
574 sorbance, since the other tested transformations did not show a strong impact on the quality of
575 the predictions. On the other hand the removal of noisy and non-informative spectral regions
576 seemed to be of fundamental importance, as reported by the participants which tested their pre-
577 diction methods before and after their removal. For example, results from Section 3.1 showed an
578 improvement of 11.6% and of 25.7% when ridge regression and LDA were respectively used in
579 combination of new polynomial variables generation after water regions removal. Again, in Sec-
580 tion 3.1.2 an improvement of the prediction performance, from 17.5% (CNN) to 20.5% (FCN),
581 after removing the water regions also when using deep learning methods is shown. Participant
582 1 also demonstrated the possibility to select the important variables directly from the spectra,
583 in fact they achieved the best prediction results using a variables selection approach starting
584 from all the spectral information (see Table 1). Variable selection was also tested in Section 3.6,
585 where a genetic algorithm was used to select a smaller subset of wavelengths without substantial
586 loss in classification performance.

587 In Section 3.3, the participants investigated the pairwise agreement among the three differ-
588 ent approaches, to calculate by comparing the observations and quantifying the percentage of

Table 10: Final confusion matrix obtained with the approach outlined in Section Sect 3.1.1.

		Actual		
		CLV	GRS	TMR
Predicted	CLV	312	55	5
	GRS	61	300	5
	TMR	6	7	326

589 classifications in agreement on the total number of observations (Table 6). Methods applied by
590 members 1 and 2 gave similar predictions (agreement of 84.21%), whereby agreement between
591 predictions from member 3 was between 70.84% (with member 2) and 72.90% (with member
592 1). Although strong, the discrepancies among the three predictions could be due to: i) the
593 different number of samples retained for model development, and ii) the different number of
594 predictors (i.e., wavelengths) used for training, considering that the first member used the en-
595 tire edited spectra, whereby the second and third applied different algorithms for wavelengths
596 selection. This investigation from the third participant permits to understand that differences
597 in data editing and different methodologies selected for the predictions, even if similar, brought
598 to consistently different class predictions.

599 A final discussion point was related to the creation of the test dataset. The dataset was
600 created by the organizers, who splitted the original dataset in 75% training and 25% test dataset,
601 considering a correct division of the classes across years into the 2 datasets. The discussion
602 revolved around whether or not divide the dataset into 75% training and 25% testing, or dividing
603 the dataset according to time components, like keeping the samples recorded in 2015 and 2016
604 into the training dataset, and the samples recorded in 2017 in the test dataset. Such temporal
605 division would permit to understand if samples recorded in previous years can predict future
606 information.

607 5 Conclusion

608 Thanks to the high number of participants, with different backgrounds, who provided their
609 prediction results, the data competition was a thought-provoking occasion to discuss some of
610 the challenges arising when analyzing spectral data and provided insightful indications.

611 As mentioned in the paper and as it was previously shown in Frizzarin et al. [2021b], the
612 stronger compositional dissimilarities between pasture-based diet and TMR-based ones induced
613 an easier discrimination between the corresponding classes. This generally led to overall good
614 performances, in terms of accuracy, for the adopted methods (see Table 9). On the other hand,
615 the distinction between milk samples originated from GRS and CLV was more challenging.
616 Nonetheless, as it is shown in Table 10, some hand-crafted strategies specifically proposed for
617 this competition showed more than promising results also when employed to detect differences
618 in the composition between distinct pasture-based feeding regimens. In particular, non-linear
619 transformations of the original wavelengths and two-steps classification approaches, outlined in
620 Section 3.1 and 3.3, seemed to be effective in solving this problem.

621 Pre-treatments were generally not beneficial for the improvement of the prediction equations,
622 while the deletion of the spectral regions related to water (with manual selection of these regions
623 or by means of automatic variable selection procedures) improved the prediction results. The
624 utilization of linear models, in particular LDA, provided some of the best results, and the
625 overall best prediction was achieved using LDA applied after wavelengths selection and random
626 polynomial generation, as it was shown in Table 9. When spectral analyses are undertaken it
627 is important to know not only the best possible statistical methods to use for the analyses, but
628 also what is the best data editing for such data.

629 **A Supplementary material**

630 **A.1 Deep neural network architecture**

Table S1: List of the deep model architectures considered in Section 3.1.2, including the number of trainable parameters for each model and the type of input data they accept.

Model Architecture	Parameters	Input Data and Shape
FCN		
- Dense layers of 1024, 512, 128, 64 and 32 units	1,785,923	- Linear, full (1060) - Linear, reduced (518)
- Output layer of 3 units		
- Dropout for dense layers, drop rate of 0.2		
- ELU activation for hidden layers		
- softmax activation for output layer		
- Adam optimiser, initial learning rate of 0.0001		
- Categorical cross entropy as loss function		
CNN		
- Convolutional layers with 32, 64 and 128 filters	55,332,419	- Squared, full (33×33) - Squared, reduced (23×23)
- Filters of shape (3, 3), (2, 2) and (2, 2)		
- Flattening layer		
- Dense layers of 512, 256, 128, 64, and 32 units		
- Output layer of 3 units		
- ELU activation for hidden layers		
- softmax activation for output layer		
- Adam optimiser, initial learning rate of 0.0001		
- Categorical cross entropy as loss function		
CNN_DILATED		
- Same architecture as CNN	41,176,643	- Squared, full (33×33) - Squared, reduced (23×23)
- Kernels built with a dilation rate of (2, 2)		

631 **A.2 Participant 3**

Table S2: Standardized canonical discriminant function coefficients of the variables selected by DA and effective size measures.

Wavenumber, cm^{-1}	Function	
	1	2
1069	2.899	0.298
1130	-3.790	0.416
1181	-2.003	5.371
1269	-7.321	-2.495
1292	10.544	-3.045
1377	-5.860	-0.482
1416	-5.885	1.267
1439	12.710	1.112
1474	-4.689	3.714
1539	-3.816	-2.385
1577	4.442	1.247
1752	11.958	6.035
2782	-1.459	0.875
2851	-15.686	-13.612
2890	16.085	3.459
2932	-4.166	0.916
Eigenvalue	1.732	0.109
& of variance	94.1%	5.9%
Canonical correlation	0.796	0.313

Table S3: Group means (centroids) for the Discriminant Functions

Diet	Function	
	1	2
CLV	0.872	0.403
GRS	0.954	-0.400
TMR	-1.895	-0.012

Table S4: Classification related statistics and leave-one-out cross-validation. ^a 71% of original grouped cases correctly classified. ^b Cross-validation is done only for those cases in the analysis. In cross-validation, each case is classified by the functions derived from all cases other than that case. 70.5% of cross-validated grouped cases correctly classified.

		Diet	Predicted Group Membership			Total
			CLV	GRS	TMR	
Original ^a	Count	CLV	629	363	83	1075
		GRS	323	668	62	1053
		TMR	39	44	942	1025
	%	CLV	58.5	33.8	7.7	100.0
		GRS	30.7	63.4	5.9	100.0
		TMR	3.8	4.3	91.9	100.0
Cross-validated ^b	Count	CLV	620	369	86	1075
		GRS	326	663	64	1053
		TMR	39	47	939	1025
	%	CLV	57.7	34.3	8.0	100.0
		GRS	31.0	63.0	6.1	100.0
		TMR	3.8	4.6	91.6	100.0

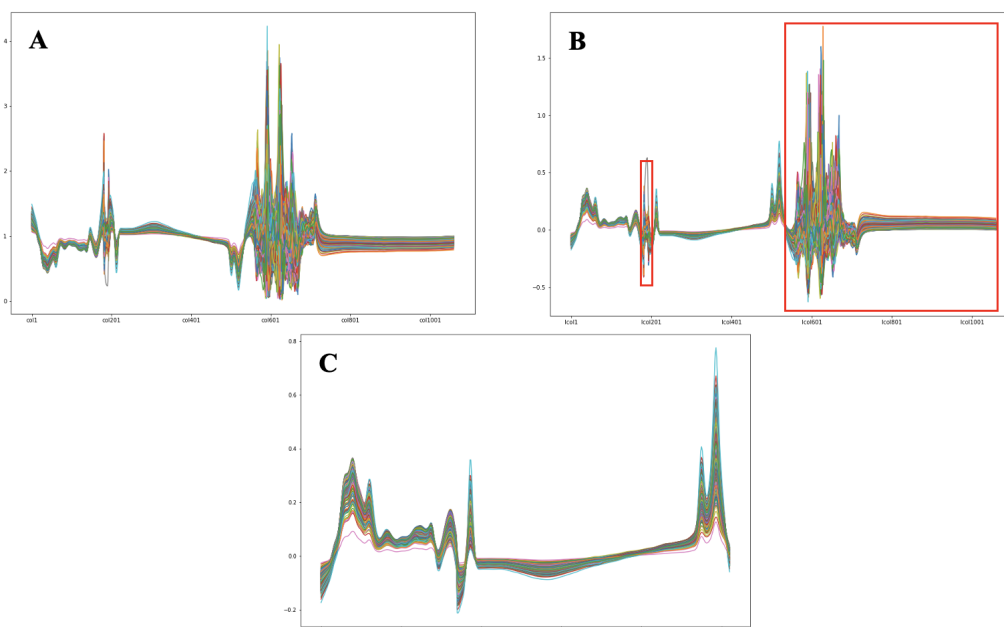


Figure S1: Line plot of raw spectra expressed in transmittance (A), conversion of raw spectra from transmittance to absorbance (B; red boxes indicate low signal-to-noise regions), and raw spectra in absorbance after noisy area removal (C).

632 Acknowledgements

633 This publication has emanated from research conducted with the financial support of Science
634 Foundation Ireland (SFI) and the Department of Agriculture, Food and Marine on behalf of
635 the Government of Ireland under grant number (16/RC/3835), the SFI Insight Research Centre
636 under grant number (SFI/12/RC/2289_P2) and the SFI Starting Investigator Research Grant
637 “Infrared spectroscopy analysis of milk as a low-cost solution to identify efficient and profitable
638 dairy cows” (18/SIRG/5562).

639 Declaration of interests

640 The authors declare that they have no known competing financial interests or personal relation-
641 ships that could have appeared to influence the work reported in this paper.

642 Data availability

643 Data used in the present paper are available upon request from the corresponding author.

644 References

- 645 Abadi, M., Agarwal, A., Barham, P., Brevdo, E., Chen, Z., Citro, C., Corrado, G. S., Davis,
646 A., Dean, J., Devin, M., Ghemawat, S., Goodfellow, I. J., Harp, A., Irving, G., Isard, M.,
647 Jia, Y., Józefowicz, R., Kaiser, L., Kudlur, M., Levenberg, J., Mané, D., Monga, R., Moore,
648 S., Murray, D. G., Olah, C., Schuster, M., Shlens, J., Steiner, B., Sutskever, I., Talwar,
649 K., Tucker, P. A., Vanhoucke, V., Vasudevan, V., Viégas, F. B., Vinyals, O., Warden, P.,
650 Wattenberg, M., Wicke, M., Yu, Y., and Zheng, X. (2016). Tensorflow: Large-scale machine
651 learning on heterogeneous distributed systems. *CoRR*, abs/1603.04467.
- 652 Abramovich, F., Sapatinas, T., and Silverman, B. W. (1998). Wavelet thresholding via a
653 Bayesian approach. *Journal of the Royal Statistical Society: Series B*, 60(4):725–749.
- 654 Agradi, S., Curone, G., Negroni, D., Vigo, D., Brecchia, G., Bronzo, V., Panseri, S., Chiesa,
655 L. M., Peric, T., Danes, D., and Menchetti, L. (2020). Determination of fatty acids profile
656 in original brown cows dairy products and relationship with alpine pasture farming system.
657 *Animals*, 10(7):1231.
- 658 Balabin, R. M. and Safieva, R. Z. (2008). Gasoline classification by source and type based on
659 near infrared (NIR) spectroscopy data. *Fuel*, 87(7):1096–1101.
- 660 Balabin, R. M. and Safieva, R. Z. (2011). Biodiesel classification by base stock type (vegetable
661 oil) using near infrared spectroscopy data. *Analytica Chimica Acta*, 689(2):190–197.
- 662 Bhati, I. and Bhattacharya, M. (2020). An IOT-based system for classification and identification
663 of plastic waste using near infrared spectroscopy. In *Proceedings of the 2nd International
664 Conference on Communication, Devices and Computing*, pages 697–703. Springer.
- 665 Bjerrum, E. J., Glahder, M., and Skov, T. (2017). Data augmentation of spectral data for con-
666 volutional neural network (CNN) based deep chemometrics. *arXiv preprint arXiv:1710.01927*.
- 667 Bonfatti, V., Di Martino, G., and Carnier, P. (2011). Effectiveness of mid-infrared spectroscopy
668 for the prediction of detailed protein composition and contents of protein genetic variants of
669 individual milk of simmental cows. *Journal of Dairy Science*, 94(12):5776–5785.
- 670 Breiman, L. (2001). Random forests. *Machine learning*, 45(1):5–32.

- 671 Brereton, R. G. (2015). The mahalanobis distance and its relationship to principal component
672 scores. *Journal of Chemometrics*, 29(3):143–145.
- 673 Chen, G., Zhang, X., Wu, Z., Su, J., and Cai, G. (2021). An efficient tea quality classification
674 algorithm based on near infrared spectroscopy and random forest. *Journal of Food Process
675 Engineering*, 44(1):e13604.
- 676 Chilliard, Y., Glasser, F., Ferlay, A., Bernard, L., Rouel, J., and Doreau, M. (2007). Diet, rumen
677 biohydrogenation and nutritional quality of cow and goat milk fat. *European Journal of Lipid
678 Science and Technology*, 109(8):828–855.
- 679 Cozzolino, D. (2012). Recent trends on the use of infrared spectroscopy to trace and authenticate
680 natural and agricultural food products. *Applied Spectroscopy Reviews*, 47(7):518–530.
- 681 De Marchi, M., Toffanin, V., Cassandro, M., and Penasa, M. (2014). Invited review:
682 Mid-infrared spectroscopy as phenotyping tool for milk traits. *Journal of Dairy Science*,
683 97(3):1171–1186.
- 684 Dempster, A., Petitjean, F., and Webb, G. I. (2020). ROCKET: exceptionally fast and accurate
685 time series classification using random convolutional kernels. *Data Mining and Knowledge
686 Discovery*, 34(5):1454–1495.
- 687 Dempster, A., Schmidt, D. F., and Webb, G. I. (2021). Minirocket: A very fast (almost) de-
688 terministic transform for time series classification. In *Proceedings of the 27th ACM SIGKDD
689 Conference on Knowledge Discovery and Data Mining*, page 248–257. Association for Com-
690 puting Machinery.
- 691 Dewhurst, R., Shingfield, K., Lee, M., , and Scollan, N. (2006). Increasing the concentrations of
692 beneficial polyunsaturated fatty acids in milk produced by dairy cows in high-forage systems.
693 *Animal Feed Science and Technology*, 131(3-4):168–206.
- 694 Domijan, K. (2018). *BKPC: Bayesian Kernel Projection Classifier*. R package version 1.0.1.
- 695 Domijan, K. and Wilson, S. P. (2011). Bayesian kernel projections for classification of high
696 dimensional data. *Statistics and Computing*, 21(2):203–216.
- 697 Ferlay, A., B, G., and Y, C. (2013). Maitrise par l’alimentation des teneurs en acides gras et en
698 composes vitaminiques du lait de vache. *INRAE Productions Animales*, 26(2):177—192.
- 699 Ferlay, A., Bernard, L., Meynadier, A., and Malpuech-Brugère, C. (2017). Production of trans
700 and conjugated fatty acids in dairy ruminants and their putative effects on human health: A
701 review. *Biochimie*, 141:107–120.
- 702 Ferragina, A., Cipolat-Gotet, C., Cecchinato, A., and Bittante, G. (2013). The use of fourier-
703 transform infrared spectroscopy to predict cheese yield and nutrient recovery or whey loss
704 traits from unprocessed bovine milk samples. *Journal of Dairy Science*, 96(12):7980–7990.
- 705 Filzmoser, P. and Gschwandtner, M. (2021). *mvoutlier: Multivariate Outlier Detection Based
706 on Robust Methods*. R package version 2.1.1.
- 707 Filzmoser, P., Maronna, R., and Werner, M. (2008). Outlier identification in high dimensions.
708 *Computational Statistics & Data Analysis*, 52(3):1694–1711.
- 709 Fleming, A., Schenkel, F., Chen, J., Malchiodi, F., Bonfatti, V., Ali, R., Mallard, B., Corredig,
710 M., and Miglior, F. (2017). Prediction of milk fatty acid content with mid-infrared spec-
711 troscopy in canadian dairy cattle using differently distributed model development sets. *Journal
712 of Dairy Science*, 100(6):5073–5081.

- 713 Friedman, J., Hastie, T., and Tibshirani, R. (2010). Regularization paths for generalized linear
714 models via coordinate descent. *Journal of Statistical Software*, 33(1):1.
- 715 Frizzarin, M., Bevilacqua, A., Dhariyal, B., Domijan, K., Ferraccioli, F., Hayes, E., Ifrim, G.,
716 Konkolewska, A., Nguyen, T. L., Mbaka, U., Ranzato, G., Singh, A., Stefanucci, M., and Casa,
717 A. (2021a). Mid infrared spectroscopy and milk quality traits: a data analysis competition
718 at the international workshop on spectroscopy and chemometrics 2021”. *Chemometrics and*
719 *Intelligent Laboratory Systems*.
- 720 Frizzarin, M., O’Callaghan, T., Murphy, T., Hennessy, D., and Casa, A. (2021b). Application
721 of machine-learning methods to milk mid-infrared spectra for discrimination of cow milk from
722 pasture or total mixed ration diets. *Journal of Dairy Science*, 104(12):12394–12402.
- 723 Geronimo, B. C., Mastelini, S. M., Carvalho, R. H., Júnior, S. B., Barbin, D. F., Shimokomaki,
724 M., and Ida, E. I. (2019). Computer vision system and near-infrared spectroscopy for identifi-
725 cation and classification of chicken with wooden breast, and physicochemical and technological
726 characterization. *Infrared Physics & Technology*, 96:303–310.
- 727 Gneiting, T. and Raftery, A. E. (2007). Strictly proper scoring rules, prediction, and estimation.
728 *Journal of the American statistical Association*, 102(477):359–378.
- 729 Hahs-Vaughn, D. L. (2016). *Applied multivariate statistical concepts*. Routledge.
- 730 Ho, P., Bonfatti, V., Luke, T., and Pryce, J. (2019). Classifying the fertility of dairy cows using
731 milk mid-infrared spectroscopy. *Journal of Dairy Science*, 102(11):10460–10470.
- 732 Hoerl, A. E. and Kennard, R. W. (1970). Ridge regression: Biased estimation for nonorthogonal
733 problems. *Technometrics*, 12(1):55–67.
- 734 Holland, J. H. (1992). *Adaptation in natural and artificial systems: an introductory analysis*
735 *with applications to biology, control, and artificial intelligence*. MIT press.
- 736 IBM Corp. (2017). *IBM SPSS Statistics for Windows, Version 25.0*. R Foundation for Statistical
737 Computing, Armonk, NY.
- 738 Ji-yong, S., Xiao-bo, Z., Xiao-wei, H., Jie-wen, Z., Yanxiao, L., Limin, H., and Jianchun, Z.
739 (2013). Rapid detecting total acid content and classifying different types of vinegar based
740 on near infrared spectroscopy and least-squares support vector machine. *Food Chemistry*,
741 138(1):192–199.
- 742 Karatzoglou, A., Smola, A., Hornik, K., and Zeileis, A. (2004). kernlab – an S4 package for
743 kernel methods in R. *Journal of Statistical Software*, 11(9):1–20.
- 744 Kassambara, A. and Mundt, F. (2020). *factoextra: Extract and Visualize the Results of Multi-*
745 *variate Data Analyses*. R package version 1.0.7.
- 746 Khuwijitjaru, P., Boonyapisompan, K., and Huck, C. (2020). Near-infrared spectroscopy with
747 linear discriminant analysis for green ‘robusta’ coffee bean sorting. *International Food Research*
748 *Journal*, 27(2):287–294.
- 749 MATLAB (2018). *version 9.4 (R2018a)*. The MathWorks Inc., Natick, Massachusetts.
- 750 McDermott, A., Visentin, G., De Marchi, M., Berry, D., Fenelon, M., O’Connor, P., Kenny, O.,
751 and McParland, S. (2016). Prediction of individual milk proteins including free amino acids
752 in bovine milk using mid-infrared spectroscopy and their correlations with milk processing
753 characteristics. *Journal of Dairy Science*, 99(4):3171–3182.

- 754 McParland, S., Lewis, E., Kennedy, E., Moore, S., McCarthy, B., O'Donovan, M., Butler, S. T.,
755 Pryce, J., and Berry, D. (2014). Mid-infrared spectrometry of milk as a predictor of energy
756 intake and efficiency in lactating dairy cows. *Journal of Dairy Science*, 97(9):5863–5871.
- 757 Meloun, M. and Militký, J. (2011). *Statistical data analysis: A practical guide*. Woodhead
758 Publishing Limited.
- 759 Mevik, B.-H., Wehrens, R., and Liland, K. H. (2020). *pls: Partial Least Squares and Principal*
760 *Component Regression*. R package version 2.7-3.
- 761 Middlehurst, M. and Bagnall, A. (2022). The freshprince: A simple transformation based
762 pipeline time series classifier. *CoRR*, abs/2201.12048.
- 763 Munera, S., Gómez-Sanchís, J., Aleixos, N., Vila-Francés, J., Colelli, G., Cubero, S., Soler, E.,
764 and Blasco, J. (2021). Discrimination of common defects in loquat fruit cv. ‘Algerie’ using
765 hyperspectral imaging and machine learning techniques. *Postharvest Biology and Technology*,
766 171:111356.
- 767 Nason, G. (2016). *wavethresh: Wavelets Statistics and Transforms*. R package version 4.6.8.
- 768 Nason, G. P. (2008). *Wavelet methods in statistics with R*. Springer.
- 769 Nguyen, T. L. and Ifrim, G. (2021). Mrsqm: Fast time series classification with symbolic
770 representations. *arXiv preprint arXiv:2109.01036*.
- 771 Nguyen, T. L. and Ifrim, G. (2022). A short tutorial for time series classification and explanation
772 with mrsqm. *Software Impacts*, 11:100197.
- 773 Oravec, M., Beganović, A., Gál, L., Čeppan, M., and Huck, C. W. (2019). Forensic classi-
774 fication of black inkjet prints using fourier transform near-infrared spectroscopy and linear
775 discriminant analysis. *Forensic Science International*, 299:128–134.
- 776 O’Callaghan, T. F., Hennessy, D., McAuliffe, S., Kilcawley, K. N., O’Donovan, M., Dillon, P.,
777 Ross, R. P., and Stanton, C. (2016). Effect of pasture versus indoor feeding systems on raw
778 milk composition and quality over an entire lactation. *Journal of Dairy Science*, 99(12):9424–
779 9440.
- 780 Pedregosa, F., Varoquaux, G., Gramfort, A., Michel, V., Thirion, B., Grisel, O., Blondel, M.,
781 Prettenhofer, P., Weiss, R., Dubourg, V., et al. (2011). Scikit-learn: Machine learning in
782 python. *Journal of Machine Learning Research*, 12:2825–2830.
- 783 Pituch, K. A. and Stevens, J. P. (2015). *Applied multivariate statistics for the social sciences:*
784 *Analyses with SAS and IBM’s SPSS*. Routledge.
- 785 R Core Team (2020). *R: A Language and Environment for Statistical Computing*. R Foundation
786 for Statistical Computing, Vienna, Austria.
- 787 Shetty, N., Difford, G., Lassen, J., Løvendahl, P., and Buitenhuis, A. (2017). Predicting methane
788 emissions of lactating danish holstein cows using fourier transform mid-infrared spectroscopy
789 of milk. *Journal of Dairy Science*, 100(11):9052–9060.
- 790 Soneson, C., Gerster, S., and Delorenzi, M. (2014). Batch effect confounding leads to strong
791 bias in performance estimates obtained by cross-validation. *PloS one*, 9(6):e100335.
- 792 Soyeurt, H., Dardenne, P., Dehareng, F., Lognay, G., Veselko, D., Marlier, M., Bertozzi, C.,
793 Mayeres, P., and Gengler, N. (2006). Estimating fatty acid content in cow milk using mid-
794 infrared spectrometry. *Journal of Dairy Science*, 89(9):3690–3695.

- 795 Soyeurt, H., Dehareng, F., Gengler, N., McParland, S., Wall, E., Berry, D., Coffey, M., and
796 Dardenne, P. (2011). Mid-infrared prediction of bovine milk fatty acids across multiple breeds,
797 production systems, and countries. *Journal of Dairy Science*, 94(4):1657–1667.
- 798 Terouzi, W., Platikanov, S., de Juan Capdevila, A., and Oussama, A. (2013). Classification
799 of olives from moroccan regions by using direct ft-ir analysis: Application of support vector
800 machines (svm). *International Journal of Innovation and Applied Studies*, 3(2):493–503.
- 801 Tibshirani, R. (1996). Regression shrinkage and selection via the lasso. *Journal of the Royal
802 Statistical Society: Series B*, 58(1):267–288.
- 803 Tiplady, K., Lopdell, T., Littlejohn, M., and Garrick, D. (2020). The evolving role of fourier-
804 transform mid-infrared spectroscopy in genetic improvement of dairy cattle. *Journal of Animal
805 Science and Biotechnology*, 11(1):1–13.
- 806 Vapnik, V. N. (1998). *Statistical Learning Theory*. Wiley.
- 807 Venables, W. N. and Ripley, B. D. (2002). *Modern Applied Statistics with S*. Springer, New
808 York, fourth edition. ISBN 0-387-95457-0.
- 809 Visentin, G., McDermott, A., McParland, S., Berry, D., Kenny, O., Brodkorb, A., Fenelon, M.,
810 and De Marchi, M. (2015). Prediction of bovine milk technological traits from mid-infrared
811 spectroscopy analysis in dairy cows. *Journal of Dairy Science*, 98(9):6620–6629.
- 812 Willighagen, E. and Ballings, M. (2022). *genalg: R Based Genetic Algorithm*. R package version
813 0.2.1.
- 814 Wright, M. N. and Ziegler, A. (2017). ranger: A fast implementation of random forests for high
815 dimensional data in C++ and R. *Journal of Statistical Software*, 77(1):1–17.
- 816 Wu, X., Fu, H., Tian, X., Wu, B., and Sun, J. (2017). Prediction of pork storage time using
817 fourier transform near infrared spectroscopy and Adaboost-ULDA. *Journal of Food Process
818 Engineering*, 40(6):e12566.
- 819 Yu, F. and Koltun, V. (2015). Multi-scale context aggregation by dilated convolutions. *arXiv
820 preprint arXiv:1511.07122*.
- 821 Zou, H. and Hastie, T. (2005). Regularization and variable selection via the elastic net. *Journal
822 of the Royal Statistical Society: Series B*, 67(2):301–320.